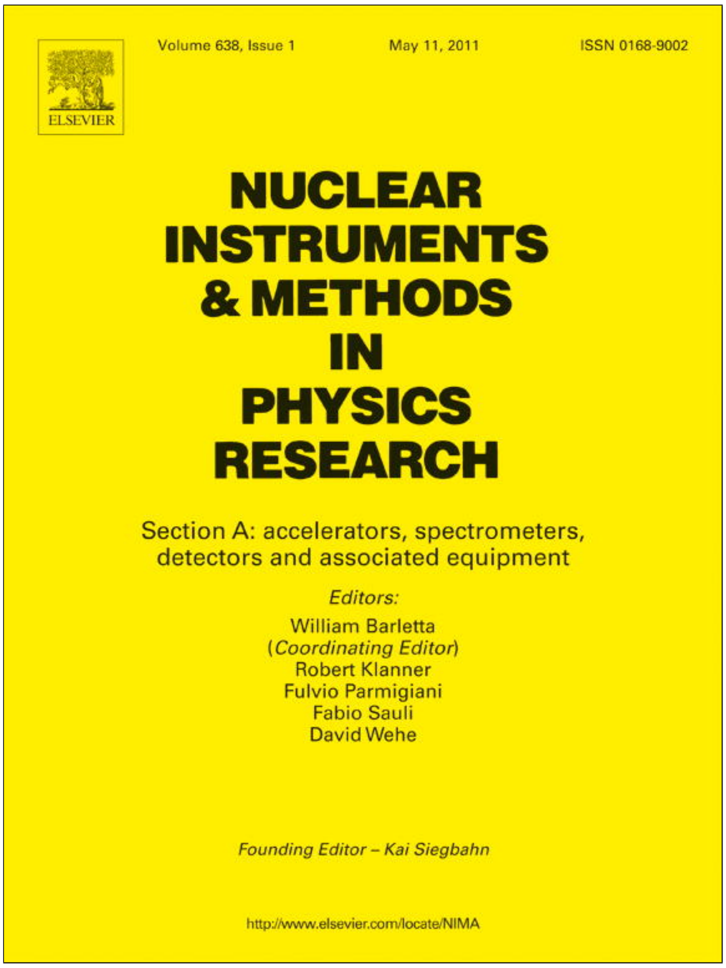
Volume 638, Issue 1
May 11, 2011
ISSN 0168-9002
ELSEVIER
NUCLEAR INSTRUMENTS & METHODS IN PHYSICS RESEARCH
Section A: accelerators, spectrometers, detectors and associated equipment
Editors:
William Barletta (Coordinating Editor)
Robert Klanner
Fulvio Parmigiani
Fabio Sauli
David Wehe
Founding Editor – Kai Siegbahn
http://www.elsevier.com/locate/NIMA

Nuclear Instruments and Methods in Physics Research A 638 (2011) 47–54

Contents lists available at ScienceDirect

Nuclear Instruments and Methods in Physics Research A

journal homepage: www.elsevier.com/locate/nima

Polarization as a tool for dual-readout calorimetry

N. Akchurin [a], F. Bedeschi [b], A. Cardini [c], M. Cascella [d], G. Ciapetti [e], D. De Pedis [f], P. Dimpfl [g], R. Ferrari [h], S. Franchino [i], M. Fraternali [i], G. Gaudio [h], J. Hauptman [g], R. Holliday [g], M. Incagli [b], F. Lacava [e], L. La Rotonda [j], S. Lee [g], M. Livan [i], E. Meoni [k], A. Negri [i], D. Pinci [f], A. Policicchio [j,1], F. Scuri [b], A. Sill [a], G. Susinno [j], S. Teknowijoyo [g], T. Venturelli [j], P. Torres [g], C. Voena [f], R. Wigmans [a,*]

[a] Texas Tech University, Lubbock, TX, USA
[b] INFN Sezione di Pisa, Italy
[c] INFN Sezione di Cagliari, Monserrato (CA) Italy
[d] Dipartimento di Fisica, Università di Pisa and INFN Sezione di Pisa, Italy
[e] Dipartimento di Fisica, Università di Roma "La Sapienza" and INFN Sezione di Roma I, Italy
[f] INFN Sezione di Roma I, Italy
[g] Iowa State University, Ames, IA, USA
[h] INFN Sezione di Pavia, Italy
[i] INFN Sezione di Pavia and Dipartimento di Fisica Nucleare e Teorica, Università di Pavia, Italy
[j] INFN Cosenza and Dipartimento di Fisica, Università della Calabria, Italy
[k] Institut de Fisica d'Altes Energies (IFAE), Universitat Autonoma de Barcelona, Bellaterra, Barcelona, Spain

ARTICLE INFO

Article history:
Received 3 December 2010
Received in revised form
22 February 2011
Accepted 22 February 2011
Available online 4 March 2011

Keywords:
Calorimetry
Cherenkov light
High-*Z* scintillating crystals
Polarization

ABSTRACT

It is shown that the signals from a high-*Z* scintillating crystal (BSO) can be separated into a scintillation and a Cherenkov component, by making use of the fact that the latter component is polarized. These studies were carried out in view of the possible application of such crystals in dual-readout calorimeters.

1. Introduction

High-density scintillating crystals have traditionally been the detectors of choice in particle physics experiments that required high-resolution electron and photon measurements. However, experiments in which such crystals serve as the electromagnetic (em) section of the calorimeter system usually have poor performance for detecting hadrons and jets [1], because of the large *e/h* ratio of the crystal section.

Recently, however, interest in using such crystals for the em section of a general-purpose calorimeter system has been renewed because of the possibility to separate their signals into components deriving from Cherenkov light and scintillation light. This would open the way to use such crystals as *dual-readout calorimeters*. Event-by-event measurements of the em fraction of showers induced by hadrons or jets, which is possible in such calorimeters, would eliminate the main reason for the poor hadronic performance [1].

In earlier papers, we have demonstrated that a significant fraction of the signal from scintillating $PbWO_4$ crystals is in fact due to Cherenkov radiation. At room temperature, Cherenkov light was measured to contribute up to 15% of the signal generated by high-energy particles traversing a $PbWO_4$ crystal [2], and this fraction increased further with the temperature [3].

Studies with a BGO crystal [4] showed that it was possible to separate the two types of light effectively by means of filters, despite the fact that Cherenkov radiation represents only a small fraction of 1% of the light produced by this bright scintillator. Large differences between the spectral properties and the time structure of the two components made this possible.

Apart from the directionality, the spectral characteristics and the time structure of the signals, there is one additional feature that might in principle be used to distinguish scintillation from

* Corresponding author. Fax: +1 806 742 1182.
E-mail address: wigmans@ttu.edu (R. Wigmans).
[1] Now at Department of Physics, University of Washington, Seattle, WA, USA.

0168-9002/$ - see front matter © 2011 Elsevier B.V. All rights reserved.
doi:10.1016/j.nima.2011.02.077

Cherenkov light, namely the fact that the latter is polarized. In this paper, we investigate the possibilities in this respect. High-energy pions are used to generate signals in a crystal, and the effects of polarization filters on the two types of light generated in this crystal are measured.

In Section 2, the crystal and the experimental setup in which it was tested are described, as well as the calibration and data analysis methods that were used. Experimental results are presented in Section 3. In Section 4, we discuss the implications of these results.

2. Equipment and measurements

2.1. Detectors and beam line

The measurements described in this paper were performed in the H8 beam line of the Super Proton Synchrotron at CERN. Our detector was a high-density (ortho) bismuth silicate ($Bi_4Si_3O_{12}$ or BSO) crystal,[2] with a length of 18 cm and a cross-section of 2.2×2.2 cm^2. This transverse dimension, relevant for our measurements, corresponds to 1.91 radiation lengths (X_0). The light produced by particles traversing this crystal [7] was read out by two photomultiplier tubes (PMTs) located at opposite ends. Hamamatsu R8900 tubes, with 10 multiplication stages and equipped with a borosilicate window and a Super Bi-Alkali photocathode, were used for this purpose.

We used two different optical transmission filters to study the crystal signals. These filters were 2.5 mm thick, made of glass. One filter, known as U330, was intended to increase the relative fraction of Cherenkov light, since it only transmitted light with short wavelengths.[3] A yellow filter (known as GG495), which transmitted only light with wavelengths longer than the 495 nm cut-off value,[4] transmitted predominantly scintillation light. These filters were mounted on the two opposite end faces of the crystal, so that light exiting from the left (the L side in Fig. 1) was essentially pure scintillation light, while the light exiting from the R side consisted predominantly of Cherenkov radiation. Because of the effects of self absorption in the crystal, more than 90% of the photoelectrons constituting the Cherenkov signals were generated by photons with wavelengths of 320–400 nm.

Both sides of the crystal were, in addition, equipped with polarization filters,[5] which were shaped to completely cover the end faces of the crystal. In order to reduce the light trapping effects of the large refractive index of BSO (n=2.06), the PMTs were coupled to the crystal by means of thin silicone "cookies".[6] These cookies provided optical contact between the crystal end face and the transmission filter (n=1.52), between the transmission and polarization filters, and between the polarization filter (n=1.49) and the PMT window.

The BSO crystal was mounted on a platform that could rotate around a vertical axis. The crystal was oriented in the horizontal plane and the rotation axis went through its geometrical center.

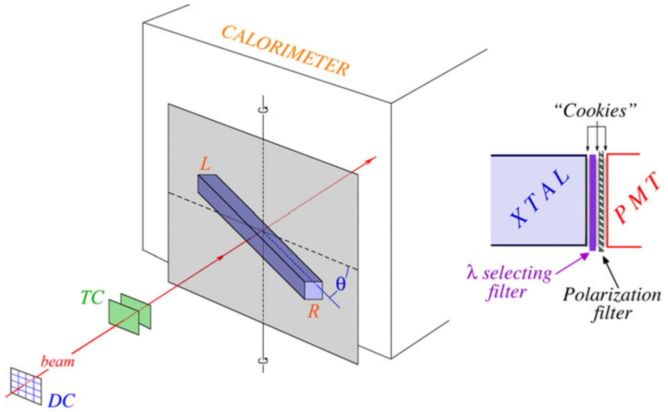

Fig. 1. Experimental setup in which the beam tests of the crystals were performed. The angle θ is negative when the crystal is oriented as drawn here. Also shown is the coupling between the crystal and the readout element (PMT). These drawings are schematic and *not* to scale.

The particle beam was also steered through this center, as illustrated in Fig. 1. The angle θ, which is frequently used in the following, represents the angle between the crystal axis and a plane perpendicular to the beam line. The angle increased when the crystal was rotated such that the crystal axis L–R approached the direction of the traveling beam particles. The crystal orientation shown in Fig. 1 corresponds to $\theta = -30°$. In many measurements, θ was chosen to be +30°, since in that case the fraction of the total generated Cherenkov light that was detected in PMT R, as well as the relative Cherenkov content of the signals from this PMT, were maximized.

Two small scintillation counters (TC) provided the signals that were used to trigger the data acquisition system. These trigger counters were 5 mm thick, and the area of overlap was 44 cm^2. A coincidence between the logic signals from these counters provided the trigger. The trajectories of individual beam particles could be reconstructed with the information provided by a small drift chamber (DC), which was installed upstream of the trigger counters. This system made it possible to determine the location of the impact point of the beam particles at the crystal with a precision of about 1 mm. About 25 m downstream of the crystal, placed behind about 20 interaction lengths of material, a 50×50 cm^2 scintillator paddle served as a muon counter. The first 10 interaction lengths consisted of the DREAM fiber calorimeter [8,9], which in this study only served to recognize and eliminate beam impurities (electrons, muons).

2.2. Data acquisition

Measurement of the time structure of the crystal signals formed a very important part of the tests described here. In order to limit distortion of this structure as much as possible, we used special 15 mm thick low-loss cables to transport the crystal signals to the counting room. Such cables were also used for the signals from the trigger counters, and these were routed such as to minimize delays in the DAQ system.[7] Other signals, *e.g.*, from the muon counter and the calorimeter, were transported through RG-58 cables with (for timing purposes) appropriate lengths to the counting room.

The data acquisition system used VME electronics. A single VME crate hosted all the needed readout and control boards. The signals from the calorimeter channels and the muon counter were integrated and digitized with a sensitivity of 100 fC/count,

[2] The term BSO is also used for other compounds consisting of bismuth, silicon and oxygen. For example, sillenite type monocrystals with composition $Bi_{12}SiO_{20}$ are commonly referred to as BSO as well [5], while the term bismuth silicate is also used for glasses [6].

[3] The transmission of U330 was ~88% at 350 nm, and ~5% at 450 nm. See for complete optical data http://www.uqgoptics.com/pdf/Hoya%20U-330.pdf.

[4] See http://www.schott.com/advanced-optics/english/download/schott_longpass_gg495_2008_e.pdf for complete optical data.

[5] HN38, a 0.28 mm thick linear polarizer made by 3 M, with a single-sheet transmission of ~25% at 350 nm and ~38% for wavelengths longer than 450 nm.

[6] Elastocil RT601, refractive index n=1.4095, transmission $\gtrsim$88% in the wavelength range of interest.

[7] We measured the signal speed to be 0.78c in these cables.

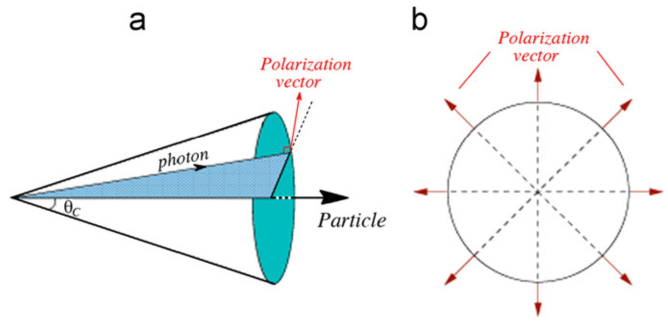

Fig. 2. Polarization of Cherenkov light emitted when a charged particle traverses a medium with refractive index n at a speed in excess of c/n. The light is emitted in a cone with angle $\theta_C = \arccos[(\beta n)^{-1}]$ (a) and is polarized with the polarization vector oriented perpendicular to this cone (b).

on 12-bit QDC V792 CAEN modules. The timing information of the tracking chambers was recorded with 1 ns resolution in a 16-bit 16-channel LeCroy 1176 TDC.

The time structure of the crystal signals was recorded by means of a Tektronix TDS 7254B digital oscilloscope,[8] which provided a sampling capability of 5 GSample/s, at an analog bandwidth of 2.5 GHz, over four input channels. For the tests described in this paper, only two channels were used to sample the signals from PMTs L and R. The oscilloscope gain (scale) was tuned such as to fully exploit the 8-bit dynamic range, *i.e.*, by choosing the sensitivity such that the overflow rate was $<1\%$.

The crystal signals were sampled every 2.0 ns, over a total time interval of 1064 ns (532 data points). The time base of the oscilloscope was started by a trigger indicating the passage of a beam particle. Our readout scheme optimized the CPU utilization and the data taking efficiency thanks to the bunch structure of the SPS cycle, where beam particles were provided to our experiment during a spill of 9.6 s, with a repetition period of 48 s. During the spill, all events were sequentially recorded in the internal memory of the scope. We were able to reach, in spill, a data acquisition rate of ~ 500 Hz, limited by the size of the internal scope buffer. No zero suppression was implemented, so that the event size was constant: ~ 1.5 MB, largely dominated by the oscilloscope data.

2.3. Experimental data and analysis methods

Cherenkov light is emitted by a medium that is traversed by a superluminal charged particle. The medium's molecules are excited and polarized in this process. They emit coherent radiation at a characteristic angle θ_C, equal to $[(\beta n)^{-1}]$, with respect to the particle track. The polarization vector of this radiation is oriented perpendicular to the direction in which the photons travel, *i.e.*, perpendicular to a cone whose central axis is the particle track and whose opening angle is θ_C. This is illustrated in Fig. 2.

In order to study the possibility to use polarization as a tool to identify Cherenkov light in the signals from our BSO crystal, we used previously exploited techniques [2,4,10] to maximize the scintillation or Cherenkov content of the light detected by the PMTs. We exploited the following differences between these components to achieve this:

(1) *Differences in directionality* [2]. Contrary to scintillation light, which is emitted isotropically, Cherenkov light is emitted at a characteristic angle ($\approx 60^\circ$ for $\beta \approx 1$) by the relativistic (shower) particles that traverse the detector. By placing the crystal at an angle $\theta = 30^\circ$, the signal measured in PMT R had the largest possible Cherenkov content.

(2) *Differences in the spectral properties* [4,10]. Cherenkov light exhibits a λ^{-2} spectrum, while the scintillation spectrum of BSO [7] peaks around 480 nm. By using a U330 filter, the signal from PMT R was strongly enriched in Cherenkov light.

(3) *Differences in time structure* [4,10]. Cherenkov light is prompt, while the scintillation mechanism in BSO is characterized by a decay time of ~ 100 ns [11]. Detailed measurement of the time structure of the L signal made it possible to remove the remaining contaminating scintillation light from the R signals.

Creating a pure scintillation signal (in PMT L) was much easier, because of the fact that scintillation photons outnumbered the Cherenkov ones by three orders of magnitude to begin with. By using a yellow transmission filter, the signals were further purified.

The measurements were performed with a 180 GeV π^+ beam. The angle θ between the crystal axis and the plane perpendicular to the beam line was varied between -50° and 50°, in steps of 5°. At each angle, 30 000 events were collected. In addition, 3000 randomly triggered events provided pedestal information. For each event, the full time structure of the signals from the two PMTs that read the two sides of the crystal was recorded, as well as the ADC and TDC data from the auxiliary detectors (fiber calorimeter, drift chambers, trigger counters, muon counters).

In this angular scan, the thickness of the crystal traversed by the pions varied between 2.2 and 3.4 cm, *i.e.*, between 0.096 and 0.149 nuclear interaction lengths. This means that in all event samples, the vast majority of the pions traversed the crystal *without* causing a nuclear interaction. In a small fraction of the events, energy deposits much larger than that caused by a mip were observed, presumably as a result of hadron showers starting in the crystal. No attempt was made to separate the (10–15%) interacting and (85–90%) non-interacting pion events.

Off-line, the drift chamber information could be used to select events that entered the crystal in a small (typically 10×10 mm^2) region located around its geometric center. The pion beam contained a few percent of muons and electrons, which could be eliminated with the help of the downstream calorimeter and muon counter.

In this paper, several different angles are mentioned. In order to avoid confusion, we list these angles, and the symbols we have used for them, below:

- The Cherenkov angle θ_C between the direction of the beam particle and the emitted Cherenkov photons. In BSO, this angle amounts to 61.0° for particles with $\beta \approx 1$.
- The angle of incidence θ between the beam direction and the BSO crystal (see Fig. 1 for the definition of this angle).
- The angle ϕ, which describes the orientation of the transmission axis of the polarization filter. This angle, which for the measurements described in this paper was 0°, 45° or 90°, is measured with respect to the horizontal plane.
- The angle ϑ is the angle between the Cherenkov photons and the horizontal plane.

2.4. Calibration of the detectors

The PMTs used in these measurements were calibrated with the 180 GeV pion beam. The calibrations were carried out at $\theta = 0$, *i.e.*, with the crystal oriented perpendicular to the beam line and the beam hitting the center of the crystal. In this geometry, the pions deposited, on average, 47 MeV in the BSO crystal, as determined with GEANT-4 Monte Carlo calculations.

For the time structure measurements, no separate calibration was performed. We only made sure that the vertical oscilloscope scale was chosen such that no significant pulse clipping occurred.

[8] http://www.tek.com/site/ps/0,,55-13766-SPECS_EN,00.html.

As the crystal was rotated to larger angles θ, the signals increased and the scale had to be adjusted, *e.g.*, from 100 to 200 to 500 mV full range.

3. Experimental results

3.1. Time structure

In order to produce Cherenkov signals that are as pure as possible, we first investigated the time structure of the light passing the U330 filter. Fig. 3a shows the average pulse shape recorded with 500 MHz digitization (*i.e.*, time intervals of 2.0 ns), for pions traversing the BSO crystal in its geometric center at $\theta = 30^\circ$.

The prompt Cherenkov component is clearly distinguished from the scintillation component, which exhibits the 100 ns decay time characteristic for this crystal. Fig. 3b shows the average time structure of the signals from light passing the yellow filter located at the *L* side of the crystal. This signal was almost exclusively composed of scintillation light. In the following, we have selected Cherenkov light by limiting the signal to the photons registered within a time interval of 20 ns, *i.e.*, from 210 to 230 ns after the start of the time base of the oscilloscope. This time interval is indicated by the gray area in Fig. 3a. As can be seen in the figure, there was some contamination from scintillation light in this signal. This contamination could be eliminated by making use of the known time structure of the scintillation signals (Fig. 3b), and the fact that the tail of the signals from PMT *R* (Fig. 3a) consisted exclusively of scintillation light as well. Based on this, we determined that $\sim 17\%$ of the signal in the gray area of Fig. 3a consisted of scintillation photons, and the Cherenkov signal was obtained by subtracting this contamination. This procedure was followed for all Cherenkov signals discussed in the following.

3.2. Position dependence

Imagine a superluminal particle that traverses the BSO crystal at an angle $\theta = 30^\circ$ (see Fig. 1). Fig. 4 illustrates some aspects of the Cherenkov light emitted by the medium traversed by this particle. Diagram (a) shows a top view of the Cherenkov cone generated from one particular point along the track, diagram (b) gives a side view, along the incident pion direction. Since $\theta_C \approx 60^\circ$, light emitted in the horizontal plane travels (approximately) perpendicular to the end face of the crystal, where PMT *R* is located.

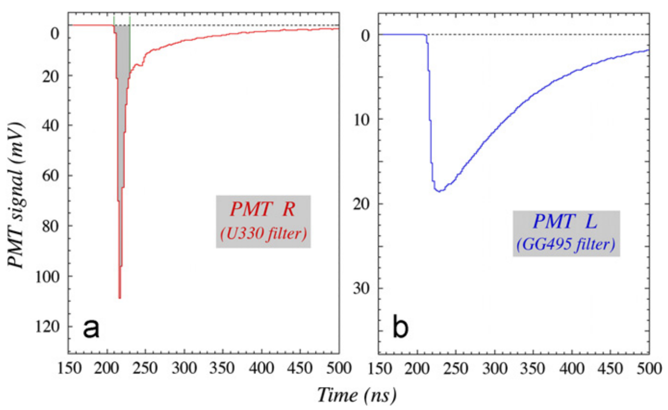

Fig. 3. Time structure of the signals generated by 180 GeV π^+ traversing a BSO crystal in its center at $\theta = 30^\circ$ and passing through a U330 optical transmission filter (a), or a GG495 yellow filter (b). The time scale describes the time passed since the start of the time base of the oscilloscope. The reflection observed in the signals from PMT *R* is caused by impedance mismatching.

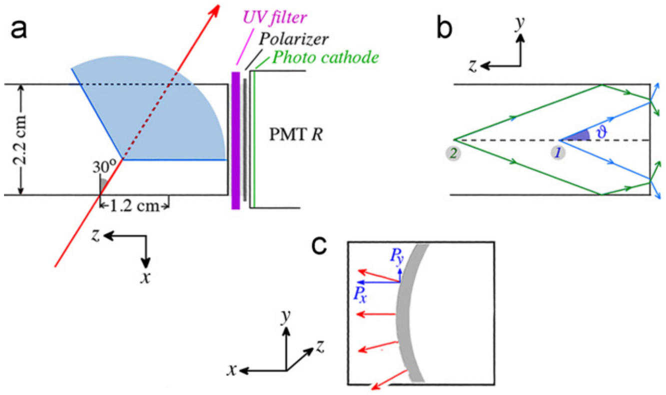

Fig. 4. Emission of Cherenkov light by particles traversing the BSO crystal at $\theta = 30^\circ$. Shown are a top view (a), a side view along the direction of the incident beam particles (b) and a view from the end face from which the Cherenkov photons exit the crystal (c). The Cherenkov cone is indicated by the shaded area in (a), and the polarization vectors of the detected Cherenkov photons by the arrows in (c). See text for further details.

Light traveling at an angle (ϑ) with the horizontal plane may also be detected in this PMT, provided that ϑ is not too large. The critical angle is determined by the indices of refraction of the BSO crystal and the cookies: $\arcsin\vartheta_{\mathrm{crit}} = 1.4095/2.06 \rightarrow \vartheta_{\mathrm{crit}} \approx 43^\circ$. However, since the refracted photons have to traverse three layers of cookies, a 2.5 mm thick UV filter, a polarization filter, as well as the glass window of the PMT before they can generate a signal (*i.e.*, photoelectrons) in the photocathode, the value is in reality quite a bit smaller, $\sim 30^\circ$. When the Cherenkov light is emitted close to the end face of the crystal (*e.g.*, from point 1 in diagram (b)), the part of the cone that is detected thus looks like the arc segment depicted in diagram (c). The polarization vector ($\vec{P}$), which is oriented perpendicular to this arc segment, points primarily in the *x* direction (Fig. 4). However, when $\vartheta \neq 0$, there is also a non-zero P_y component. But even in the most extreme cases, *i.e.*, with ϑ close to the critical value, this P_y component is less than half as large as P_x. So if we were to combine the polarization vectors of all Cherenkov photons detected in this case, the *x* component of the resulting vector would be substantially larger than the *y* component.

When the Cherenkov light is produced farther away from the crystal end face, *e.g.*, in point 2 (diagram (b)), then part of the photons generated at $\vartheta \neq 0$ will be reflected off a crystal surface before reaching the PMT. In general, reflection off a dielectric surface changes the polarization of the incoming light, since the *s* and *p* components of that light are affected differently. However, because of the large refractive index, total internal reflection in the BSO crystal is limited to a small fraction of the available phase space, which limits the scope of the effects. For example, in the setup discussed here, where beam particles traverse the crystal at $\theta = 30^\circ$, reflected light contributing to the Cherenkov signals is composed of photons that travel at an angle smaller than 29° with the horizontal plane, while the projection of their momentum vector on the horizontal plane makes an angle smaller than 5° with the longitudinal crystal axis.

As the impact point of the beam moves away from PMT *R*, the relative contributions of unreflected and reflected light to the Cherenkov signals change, in favor of the latter. The radius of the arc segment on the crystal end face resulting from the unreflected light (Fig. 4c) increases, thus increasing the polarization of that signal component. On the other hand, multiple reflections may decrease the polarization of the signal from reflected light. These combined effects determine the effective polarization of the overall signal.

We now turn to the experimental data, and in particular to the measurements of the Cherenkov signals as a function of the distance the light had to travel to PMT *R*. In order to maximize the strength of these signals, the BSO crystal was oriented at $\theta = 30^\circ$. Measurements were performed with the polarization filters in two orientations: With the transmission axis of the polarization filter parallel to the polarization direction of the Cherenkov photons, *i.e.*, in the horizontal plane (Fig. 4c), and rotated by 90°, *i.e.*, with the transmission axis in the vertical plane.

Fig. 5 shows that this rotation had a large effect on the Cherenkov component of the signals from PMT *R*, while leaving the scintillation component practically unchanged. When the beam traversed the crystal at $\theta = 30^\circ$, the Cherenkov component was reduced by a factor of about 3.5 as a result of the rotation of the transmission axis of the polarization filter from the horizontal to the vertical plane.

This confirms that the polarization vectors of the detected Cherenkov photons were indeed predominantly pointing in the x direction (Fig. 4c).

In the following, we refer to the signals measured with the polarization filter in place using the angle ϕ of the transmission axis with respect to the horizontal plane. For example, *C*0 is the Cherenkov signal measured with the transmission axis horizontal, *S*90 is the scintillation signal with the transmission axis vertical.

The signal ratio *C*0/*C*90 is shown in Fig. 6 as a function of the impact point of the beam particles in the crystal. The position of the light detectors is indicated in this figure. The ratio *C*0/*C*90 is approximately constant over most of the entire length of the crystal, indicating that the makeup of the polarization vectors of the detected Cherenkov photons did not change by much as the distance these photons had to travel before reaching the PMT increased. However, this changed when the impact position of the beam particles approached the end face of the crystal to the point that the last part of the trajectory passed through the area in between the polarization filter and the photocathode of the PMT (see Fig. 4a). In that case, Cherenkov light generated in that area, *e.g.*, in the cookie or the glass of the PMT window, did not pass the polarization filter, and rotating that filter did therefore not have an effect on that portion of the signal. Fig. 4a shows that the transverse distance traversed by a beam particle entering at $\theta = 30^\circ$ is about 1.2 cm. Together with the width of the beam spot (0.4 cm for this part of our studies), we should thus expect the signal ratio *C*0/*C*90 to decrease from its asymptotic value (~ 3.5) to 1.0 over a shift in the impact point of about 1.2+0.4=1.6 cm. This is in good agreement with the experimental observations.

We checked that the observed effects are indeed due to polarization by measuring the effects of rotating the polarization filter on the scintillation signals, *i.e.*, the signals from PMT *L*. The

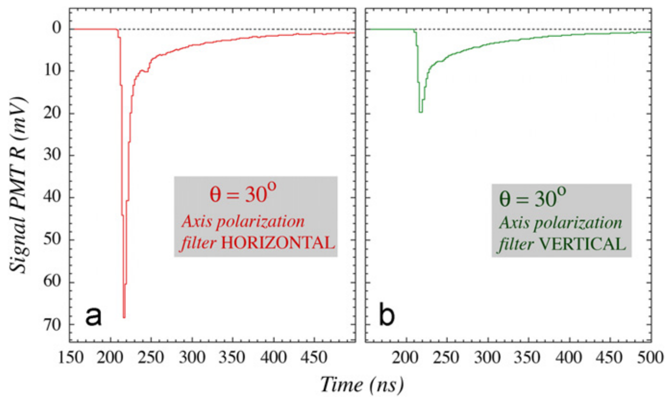

Fig. 5. Average time structure of the signals generated by 180 GeV π^+ traversing a BSO crystal in its center at $\theta = 30^\circ$ and passing through a U330 optical transmission filter, followed by a polarization filter. The transmission axis of the latter filter is either oriented horizontally (a) or vertically (b). The zero of the time scale is given by the start of the time base of the oscilloscope.

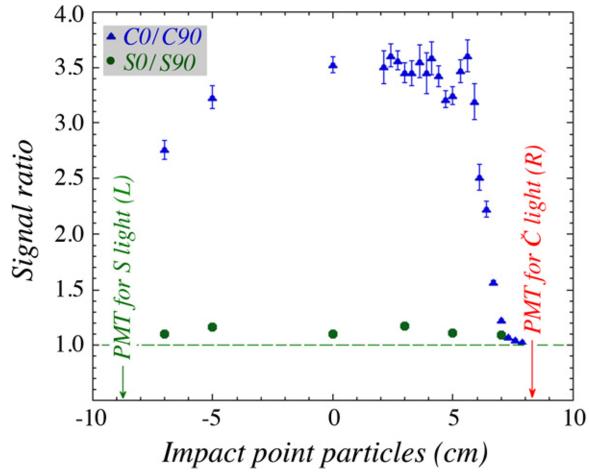

Fig. 6. Ratio of the signals measured with the transmission axis of the polarization filters in the horizontal plane and in the vertical plane, respectively. The signals were generated by 180 GeV $\pi+$ beam particles traversing the BSO crystal at $\theta = 30^\circ$. Results are given separately for the Cherenkov and scintillation signals, as a function of the impact point of the particles. The error bars are statistical only, and dominated by the uncertainty in the subtraction of the contaminating scintillation light to the Cherenkov signals. The position of the two light detectors is indicated.

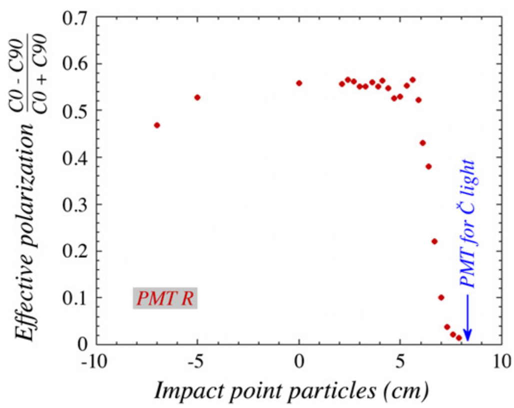

Fig. 7. The effective polarization of the Cherenkov light produced by 180 GeV π^+ beam particles traversing the BSO crystal at $\theta = 30^\circ$. See text for details.

results for the signal ratio *S*0/*S*90 are represented by the circles in Fig. 6. The orientation of the filter had no significant effect on these signals.

These results clearly prove that the Cherenkov light detected in PMT *R* was polarized, in the horizontal plane. In order to quantify these results further, we determined the *effective polarization*, by calculating the ratio of the difference and the sum of the signals measured with the two orientations of the polarization filter. This way of representing the data has the advantage that one could also quantify the effects of polarization for rotation over an angle $\Delta\phi$ other than 90°. The results shown in Fig. 7 indicate that the effective polarization of the Cherenkov light was quite substantial, more than 50% when the light was produced 2–10 cm away from the PMT that detected it.

When the distance the Cherenkov light had to travel to reach PMT *R* increased to more than 10 cm, the effective polarization was observed to decrease.[9] This is presumably a consequence of the depolarizing effect of multiple reflections.

[9] This was in particular also obvious when detecting Cherenkov light produced at the *anti-Cherenkov angle* ($\theta = -30^\circ$), in which case the Cherenkov photons had to travel 27 cm before reaching PMT *R*. See Fig. 10 for details.

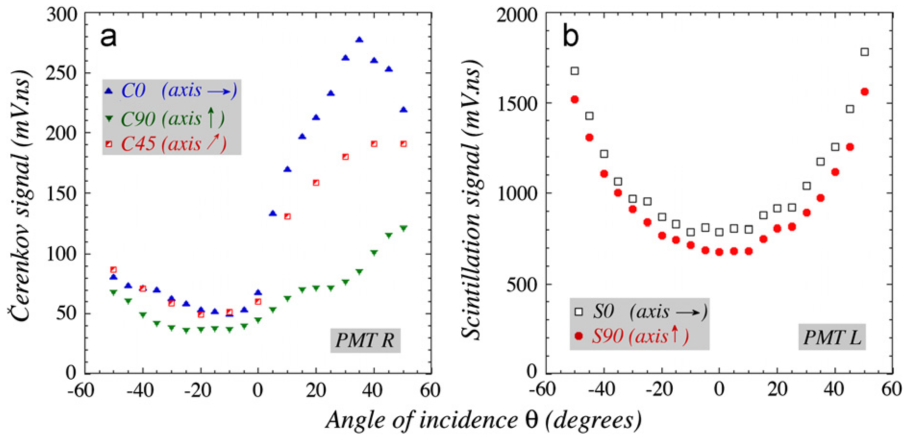

Fig. 8. Angular dependence of the polarization effects. Shown is the average amplitude of the signals generated by 180 GeV π^+ beam particles as a function of the angle θ at which these particles traverse the BSO crystal. Results are given for the Cherenkov signals, with the transmission axis of the polarization filter oriented in the horizontal plane (*C*0), the vertical plane (*C*90), or at an intermediate position (*C*45), and for the scintillation signals with the transmission axis in the horizontal (*S*0) or vertical (*S*90) plane.

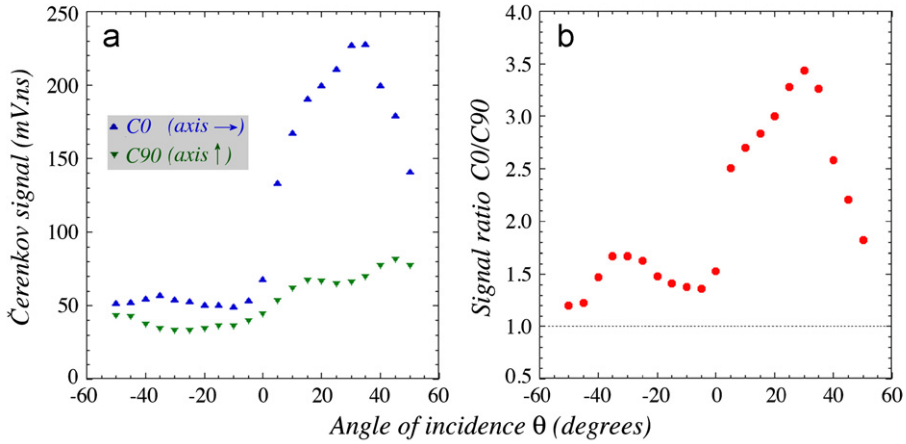

Fig. 9. The effect of rotating the transmission axis of the polarization filter from the horizontal plane to the vertical plane on the amplitude of the Cherenkov signals, as a function of the angle of incidence θ of the 180 GeV π^+ beam particles. In order to eliminate the trivial contribution of the changing path length of the beam particles in the BSO crystal, the signals have been multiplied by cosθ. Shown are the average signals for the two orientations of the polarization filter (a) and the ratio of these signals (b).

3.3. Angular dependence

In a separate study, we investigated the effect of the angle of incidence θ on the polarization of the detected Cherenkov light. The 180 GeV π^+ beam was steered into the geometric center of the BSO crystal in these measurements. The angle θ was varied between -50° and $+50^\circ$, in steps of 5°.

Results of these measurements are shown in Fig. 8, where the average amplitude of the following signals is plotted as a function of the angle of incidence θ:

- The Cherenkov signal with the transmission axis in the horizontal plane (*C*0).
- The Cherenkov signal with the transmission axis in the vertical plane (*C*90).
- The Cherenkov signal with the transmission axis at 45° with both planes (*C*45).
- The scintillation signal with the transmission axis in the horizontal plane (*S*0).
- The scintillation signal with the transmission axis in the vertical plane (*S*90).

The Cherenkov nature of the light detected in PMT *R* is very clear from the θ asymmetry of the signals. Whereas the angular distribution of the scintillation signals in PMT *L* is symmetric around $\theta = 0$, and only exhibits the $1/\cos(\theta)$ dependence expected on the basis of the increased path length of the beam particles through the crystal, the amplitudes of the signals detected in PMT *R* are considerably larger for $\theta > 0$ than for $\theta < 0$, especially near the (complement of the) Cherenkov angle.[10] The latter effect is much more pronounced for the measurements in which the transmission axis of the filter was oriented in the same (horizontal) plane as the polarization vector of the Cherenkov photons (*C*0) than for other orientations of this axis (*C*45,*C*90). The orientation of the polarization filter had no significant effect on the scintillation signals.[11]

The effects of the polarization filter on the Cherenkov signals are further detailed in Fig. 9. In order to eliminate the effects of the increased path length of the pions through the BSO crystal, all signals have been multiplied by a factor cosθ. The resulting

[10] The index of refraction of BSO is 2.06, leading to a Cherenkov angle $\arccos(1/2.06) = 61^\circ$. Therefore, one expects the maximum signal amplitude for $\theta \sim 29^\circ$.

[11] The fact that the scintillation signals were, on average, about 10% larger for the horizontal orientation of the polarization axis is most likely the result of differences in the quality of the optical coupling and/or oscilloscope baseline effects. We conclude that from the fact that the differences were significantly smaller when this measurement was recently repeated (see also Fig. 11, where the differences for $\theta < 0$ were much smaller). Angular independent effects of this magnitude may of course also have affected the Cherenkov results somewhat.

(normalized) Cherenkov signals are shown in Fig. 9a, for the two orientations of the polarization filter (*C*0 and *C*90). Interestingly, the effects of the polarization filter are not limited to the angular region near $\theta = 90^\circ - \theta_C$, but also show up near $\theta = -30^\circ$. The signal detected in this case contained Cherenkov light that was reflected against the crystal end connected to PMT *L*, and detected at the opposite end by PMT *R* intended for the Cherenkov signals.

Evidence for the detection of Cherenkov light at the "anti-Cherenkov angle" was observed earlier in studies of molybdenum-doped $PbWO_4$ crystals [10], where the origin of a (much smaller) bump at this angle was established from the fact that this signal was delayed by a few nanoseconds with respect to the (much larger) signal observed at $\theta = 30^\circ$. This delay was consistent with the extra time needed for the light to make a roundtrip in the crystal.

The effect of the polarization filter on Cherenkov light emitted in the "opposite" direction is especially evident in Fig. 9b, where the ratio of the Cherenkov signals measured with the transmission axis of the polarization filter oriented horizontally and vertically is plotted as a function of the angle of incidence of the beam particles. Part of the reason for the enhancement of this effect is the fact that at the angles where the Cherenkov signal measured with the transmission axis oriented horizontally (*C*0) is strongest, *i.e.*, near $\theta = 90^\circ - \theta_C$ and $\theta = \theta_C - 90^\circ$, the signal measured with the axis vertically (*C*90) exhibits a significant local dip. Apparently, the blocking effect of the polarization filter works best when the electric field vector of the photons is predominantly oriented perpendicular to the transmission axis, just as the transmission is optimal when the field vector is aligned with this axis.

Just as before, we have quantified the results of these angular scans in terms of the effective polarization of the observed Cherenkov signals, by determining the ratio of the difference and the sum of the signals measured when the transmission axis of the polarization filter was rotated from the vertical direction ($\phi = 90^\circ$) to another ϕ value. The results are shown in Fig. 10, for measurements in which the beam particles traversed the BSO crystal in its geometric center. The maximum effective polarization was measured to be $\sim 55\%$ for a rotation from $\phi = 90^\circ$ to $\phi = 0^\circ$, *i.e.*, bringing the transmission axis in the horizontal plane, for an angle of incidence $\theta \sim 30^\circ$. For a rotation of the transmission axis to $\phi = 45^\circ$, the effective polarization was measured to be $\sim 40\%$ at this angle of incidence. For light produced by particles in the crystal oriented at the "anti-Cherenkov angle" and detected in PMT *R*, effective polarizations of 20–25% were measured.

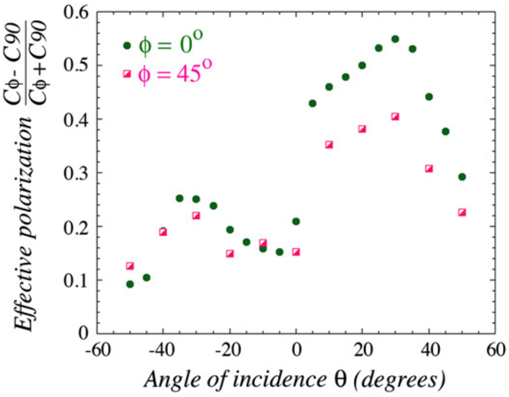

Fig. 10. The effective polarization of the Cherenkov light produced by 180 GeV $\pi+$ beam particles traversing the BSO crystal, as a function of the angle of incidence θ, in the center of the crystal. Results are given for a rotation of the transmission axis of the polarization filter by 90° with respect to the vertical plane (maximum polarization) and for a rotation by 45°. See text for details.

3.4. The integrated signals

All measurements described in the previous subsections used the time structure to determine the Cherenkov content of the signals from PMT *R*. In this section, we present the results from a study in which the integrated charge contained in these signals represented the experimental information.

Fig. 11 shows the integrated signals from PMTs *L* and *R* as a function of the angle of incidence θ of the beam particles. The signals from PMT *R* are given for the usual two orientations of the transmission axis of the polarization filter: in the horizontal plane (*C*0) and in the vertical plane (*C*90). The latter signal exhibits the same $1/\cos(\theta)$ (path length) trend as the (unpolarized) scintillation light, whereas the *C*0 signal also here shows significant polarization effects of the Cherenkov component of the light transmitted by the U330 filter. However, a comparison with Fig. 8 illustrates the importance of the time information of the signals for an analysis such as the one described in this paper.

3.5. Event-by-event information

All results shown in the previous subsections concern the average signals for event samples containing typically of the order of 10 000 pions traversing the crystal. However, if one wanted to use polarization as a tool to distinguish between scintillation and Cherenkov light, the information for individual events would have to be relied upon.

Fig. 12 shows scatter plots relating the signals measured at the two ends of the crystal for $\theta = 30^\circ$. Results are given for measurements in which the transmission axis of the polarization filter installed at the Cherenkov side was oriented in the horizontal plane (Fig. 12a) and in the vertical plane (Fig. 12b). There is clearly a correlation between the *S* and *C* signals. It is also clear that the *C*0 signals are, on average, considerably larger than the *C*90 ones. However, there are also very large event-to-event fluctuations.

The average energy deposited by a 180 GeV π^+ traversing this crystal at 30° was found, from GEANT4 Monte Carlo simulations, to be 65 MeV. The most probable energy deposit was 23 MeV. In a separate study [7], we measured the Cherenkov light yield in this setup to be 48 photoelectrons per GeV. This means that the

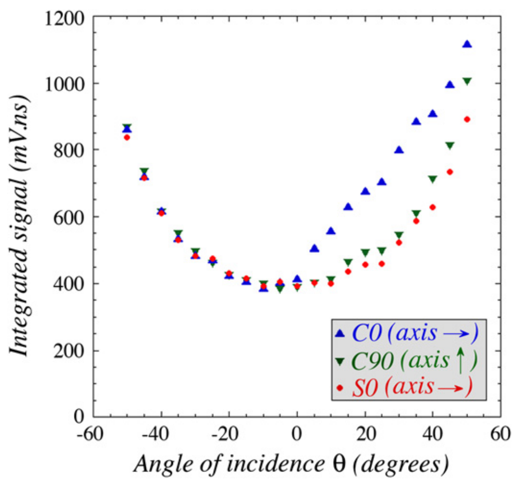

Fig. 11. Angular dependence of the polarization effects for the time integrated signals from the BSO crystal. Shown is the average integrated charge of the signals generated by 180 GeV π^+ beam particles as a function of the angle of incidence θ. Results are given for the signals from PMT *R*, with the transmission axis of the polarization filter oriented in the horizontal plane (*C*0), or the vertical plane (*C*90), and for the scintillation signals from PMT *L* with the transmission axis in the horizontal plane (*S*0).

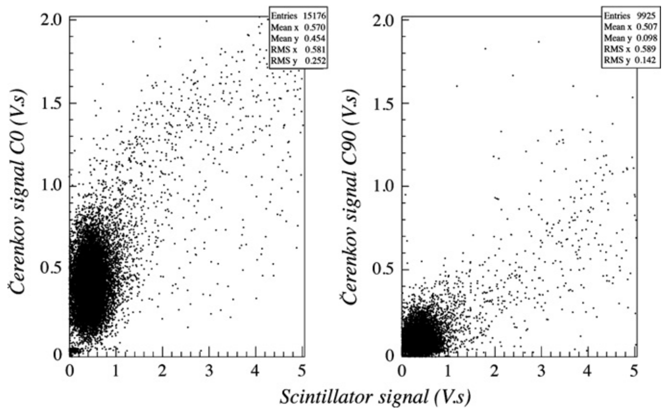

Fig. 12. Scatter plots relating the signals observed at the two ends of the crystal for 180 GeV π^+ pions crossing the crystal at $\theta = 30^\circ$. Results are given for measurements in which the transmission axis of the polarization filter was oriented in the horizontal plane (a) and in the vertical plane (b).

average C0 signal consisted of only 3 photoelectrons, and that the full vertical scale in Fig. 12 corresponds to about 20 photoelectrons. In this study, the large event-to-event fluctuations are thus clearly dominated by Poisson fluctuations in the number of (Cherenkov) photoelectrons.

It would be interesting to measure the event-to-event fluctuations for much larger energy deposits, *e.g.*, in electron showers. Of course, as these showers develop, the shower particles and thus the Cherenkov light they emit gradually become more isotropic, thus reducing the effective polarization. We plan to report on these effects in a future paper.

4. Conclusions

There is an increased interest to use high-Z crystals as the em section of calorimeter systems that are also capable of measuring hadronic showers with excellent precision. To that end, it is necessary to separate the signals from such crystals into Cherenkov and scintillation components. In this paper, we have demonstrated that the fact that Cherenkov light is polarized could in principle be used for that purpose. In addition to previously studied differences in directionality [2], spectral characteristics [4] and time structure [10], polarization thus provides a fourth tool in this respect. However, it should be emphasized that not all these tools are equally useful in practical calorimeters. For example, in 4π calorimeters designed for a colliding beam experiment, it is almost imperative that this calorimeter consist of towers pointing to the interaction vertex. In such a geometry, it is almost impossible to exploit the fact that the Cherenkov light produced by the showers is directional, as opposed to the isotropically emitted scintillation light. Different filters used to read out the crystals from the upstream and downstream ends are much more promising in this context, especially if the time structure of these signals is measured as well. Installing polarization filters with the transmission axes orientated perpendicular to each other on the upstream and downstream readout channels might provide additional separation power in such a geometry. In fixed-target experiments, one has many more options in designing the calorimeter system, and thus the possibilities to use the mentioned methods for extracting a Cherenkov signal from the (typically overwhelming) scintillation background are more numerous. The polarization of the Cherenkov light might offer additional possibilities in this respect.

Acknowledgments

We thank CERN for making particle beams of excellent quality available. We thank Dr. Hajime Shimizu for lending us the BSO crystals used for the study described in this paper. This study was carried out with financial support of the United States Department of Energy, under Contract DE-FG02-07ER41495, and by Italy's Istituto Nazionale di Fisica Nucleare and Ministero dell'Istruzione, dell'Università e della Ricerca.

References

[1] R. Wigmans, N. J. Phys. 10 (2008) 025003.
[2] N. Akchurin, et al., Nucl. Instr. and Meth. A 582 (2007) 474.
[3] N. Akchurin, et al., Nucl. Instr. and Meth. A 593 (2008) 530.
[4] N. Akchurin, et al., Nucl. Instr. and Meth. A 595 (2008) 359.
[5] E.O. Klebanskiĭ, et al., Phys. Solid State 41 (1999) 913.
[6] Z. Yang, Q. Zhang, Z. Jiang, J. Phys. D: Appl. Phys. 38 (2005) 1461.
[7] N. Akchurin, et al., Nucl. Instr. and Meth., accepted for publication.
[8] N. Akchurin, et al., Nucl. Instr. and Meth. A 536 (2005) 29.
[9] N. Akchurin, et al., Nucl. Instr. and Meth. A 537 (2005) 537.
[10] N. Akchurin, et al., Nucl. Instr. and Meth. A 604 (2009) 512.
[11] H. Shimizu, et al., Nucl. Instr. and Meth. A 550 (2005) 258.